Journal of Alloys and Compounds 509 (2011) 820–826

Contents lists available at ScienceDirect

Journal of Alloys and Compounds

journal homepage: www.elsevier.com/locate/jallcom

Formation of ZnO nanorod arrays on polytetraflouroethylene (PTFE) via a seeded growth low temperature hydrothermal reaction

W.K. Tan [a], Khairunisak Abdul Razak [a,*], K. Ibrahim [b], Zainovia Lockman [a,*]

[a] School of Materials and Mineral Resources Engineering, Engineering Campus, Universiti Sains Malaysia, 14300 Nibong Tebal, Penang, Malaysia
[b] School of Physics, Universiti Sains Malaysia, 11800 Penang, Malaysia

ARTICLE INFO

Article history:
Received 11 August 2010
Received in revised form
17 September 2010
Accepted 19 September 2010
Available online 25 September 2010

Keywords:
Nanostructured materials
Thin films
Electrode materials
Crystal growth

ABSTRACT

ZnO nanorod arrays were formed by a low temperature hydrothermal process on seeded polytetraflouroethylene (PTFE) sheets. The seed layer was formed using thermal oxidation of a thin evaporated Zn film on the PTFE sheet at 300 °C in air for 10 min. The formation of ZnO nanorod arrays in the hydrothermal reactive bath consisting of hexamethylamine (HMT) and Zn ions occurred via the reaction of hydroxyl ions released during the thermal degradation of HMT with the Zn ions. The seed layer provided a template for the nucleation of the ZnO and HMT which also acted as a chelating agent that promoted growth of the ZnO along the *c*-axis, leading to the formation of exclusively (0 0 2) ZnO nanorods. The effect of exposure time of the seeded PTFE to the reactive solution on the formation of the nanorods was investigated. Well aligned, relatively uniform tapered 300 nm long nanorods can be formed after 8 h of exposure. Longer exposure times to 24 h resulted in the formation of more uniform nanorods with base diameter averaged of ~100 nm and the tip diameter of ~50 nm. XRD analysis showed that the ZnO nanorod array had a hexagonal wurtzite structure. This result is in agreement with HR-TEM observations and Raman scattering analysis. Photoluminescence study showed that a strong UV emission peak was obtained at 380 nm and a small peak at 560 nm, which is associated with green emission. The optical band gap measured from these plots was at 3.2 eV on average.

1. Introduction

Flexible display panels have recently gained tremendous attention in the display industry because they are promising for lightweight portable devices, such as digital cameras, personal digital assistants, remote controls and mobile phones [1,2]. In a flexible display panel, an electrode layer is an important component because it ensures the effectiveness of the devices [3]. The electrode is a thin film of transparent conducting oxide (TCO), such as In:SnO_2 (ITO) or ZnO deposited on a polymeric substrate. Plastic displays are preferred to glass displays because they are more flexible, much lighter, more robust and less rigid. Furthermore, plastic displays can be produced in a large scale for large volume roll-to-roll production. The commonly used polymeric substrates for the production of plastic displays include polytetrafluoroethylene (PTFE), polycarbonate (PC), polyarylate (PAR), polyestersulfone, (PES), polyimide (PI), polyethylene terephthalate (PET) and polymethyl methacrylate (PMMA) [4]. The TCO used for the plastic displays must have high conductivity and transparency, and ITO is the TCO of choice; however, ZnO is as outstanding a conducting oxide as ITO.

In recent years, there has been a growing interest in the formation of one-dimensional (1D) ZnO nanorod arrays for various optoelectronic applications [5]. It is inferred that ZnO nanorod arrays have excellent conductivity and transparency due to the neat assembly of the oxide, which could reduce the scattering areas significantly. One-dimensional ZnO nanorod arrays are typically synthesised in a gas phase by a vapour–liquid–solid process or a vapour–solid process like chemical vapour deposition or pulsed laser deposition. Although these processes could be adopted for high-quality single crystal nanorods, the strict substrate requirements, due to the high temperature processes, could impede the formation of ZnO nanorods on polymeric substrates.

In this work, PTFE was chosen as the polymeric substrate for ZnO nanorod array growth. PTFE is known for its outstanding properties: high dielectric strength, low dissipation factor, high surface electrical resistivity, chemical resistivity and excellent flexibility [6]. The high melting point of PTFE (~450 °C) enables the formation of a ZnO seed layer via the oxidation of an ultrathin Zn layer on the PTFE using the hydrothermal reaction at 80 °C. In this work, we obtained a ZnO nanorod array on a thermally oxidised Zn film on PTFE. The thermally oxidised substrate provides a good seed layer for the formation of nanorod arrays. In a wet chemical method, post-annealing heat treatment is often required to induce crys-

* Corresponding authors.
E-mail addresses: khairunisak@eng.usm.my (K.A. Razak), zainovia@eng.usm.my (Z. Lockman).

0925-8388/$ – see front matter © 2010 Elsevier B.V. All rights reserved.
doi:10.1016/j.jallcom.2010.09.099

tallisation [7]. However, in this work, the ZnO nanorod arrays are highly crystalline and well aligned without a post-annealing process. Though a few works have been reported on the formation of TCO on polymeric substrates for plastic displays [8], not many have reported on the formation of ZnO nanorod arrays by the hydrothermal reaction on a seeded PTFE sheet. It is therefore of interest to study the growth mechanism of nanorod array growth on such a substrate. Morphologies of the nanorods formed were monitored as a function of reaction time, and the mechanism of formation is discussed in this work.

2. Experimental procedure

A PTFE sheet with thickness of ~0.1 mm was cleaned ultrasonically with acetone for 15 min before being placed in a thermal evaporator chamber (Edward Auto 306). To deposit the Zn film on the PTFE sheet, 99.99% pure zinc granules were used as the Zn source. The pressure of the evaporator chamber used for the thermal evaporation was 5×10^{-5} Torr. After evaporation, the PTFE sheet was covered with a 400 nm thin Zn film. The Zn coated PTFE sheet was then subjected to thermal oxidation at 300 °C and 400 °C for 10 min. Oxidation was carried out either in air or in oxygen. To view the surface morphology of the oxidised sample, a field emission scanning electron microscope ZEISS SUPRA 35VP FESEM (with Energy Dispersive X-ray (EDX)) was used. After deciding on the feature of the surface oxide best used as the seed layer for hydrothermal reaction, the sample was then placed in an autoclave filled with a 1:1 ratio of 0.1 M $Zn(NO_3)_2$ and 0.1 M hexamethylamine $(CH_2)_6N_4$ (HMT) hydrothermal reactive solution. A seed layer must comprise of uniformly distributed ZnO grains in nanoscale. From this work, oxidation in air was found to form an appropriate seed layer for the ZnO nanorods to grow. The hydrothermal reaction was investigated at time varied from 4 h to 24 h. After the hydrothermal reaction was completed, the samples were cleaned and subjected to morphological and structural characterizations. FESEM was used to investigate the nanostructure formation and to observe further insight into the nanorods produced, high-resolution transmission electron microscopy (HR-TEM) observation was carried out using a Philips Tecnai 200 kV. An X-ray diffractometer (Bruker AXS D8 Advance XRD) with CuK_α radiation was used for phase identification. Raman spectroscopy was used to analyse the prepared samples. The photoluminescence (PL) studies were performed using a Jobin YvonHR 800 UV.

3. Results and discussion

3.1. Structure of the substrate

The surface morphology of the Zn film before oxidation process is shown in Fig. 1(a). The Zn formed as hexagonal grains with sizes ranging from 200 to 500 nm. Judging from the shape of the grains, it is assumed that the Zn formed with a majority of (0 0 0 1) grains growing parallel to the surface of the substrate. Fig. 1(b) is a higher magnification image of the sample showing that the individual hexagonal grains were comprised of smaller grains, also with a hexagonal shape with diameter of ~100 nm, as marked in the figure. The Zn film had good adherence to the PTFE sheet. To measure the thickness of the Zn film on the PTFE sheet, the sample was bent and viewed under FESEM. Fig. 1(c) shows a representative cross sectional morphology of the Zn film, demonstrating that the thickness of the film is 400 nm on average.

Upon oxidation in air at 400 °C, the shape of the surface grains did not change very much, as shown in Fig. 2(a). Fig. 2(b) shows a higher magnification image of the sample. Oxidation in oxygen changed the surface morphology drastically into whisker-like oxides protruding around the grain boundaries of the hexagonal grains (Fig. 2(c)). The formation of this kind of morphology has been reported by Li et al. [9] for vapour–solid growth of the oxide from hexagonal Zn grains with (0 0 0 1) face parallel to the substrate. The (0 0 0 1) Zn face did not oxidise very fast in comparison to side walls of the hexagonal Zn [10]. Due to the slow oxidation rate of the (0 0 0 1) face, the surface atoms are thought to sublime, forming vapour of Zn. A temperature of 400 °C is high enough to allow a certain degree of sublimation of Zn as Zn melts at 419 °C. It is therefore inferred that when Zn sublimes, the Zn vapour forms Zn clusters in air in the vicinity of the grains upon reaching supersaturation, and ZnO forms in the presence of atmospheric oxygen. The

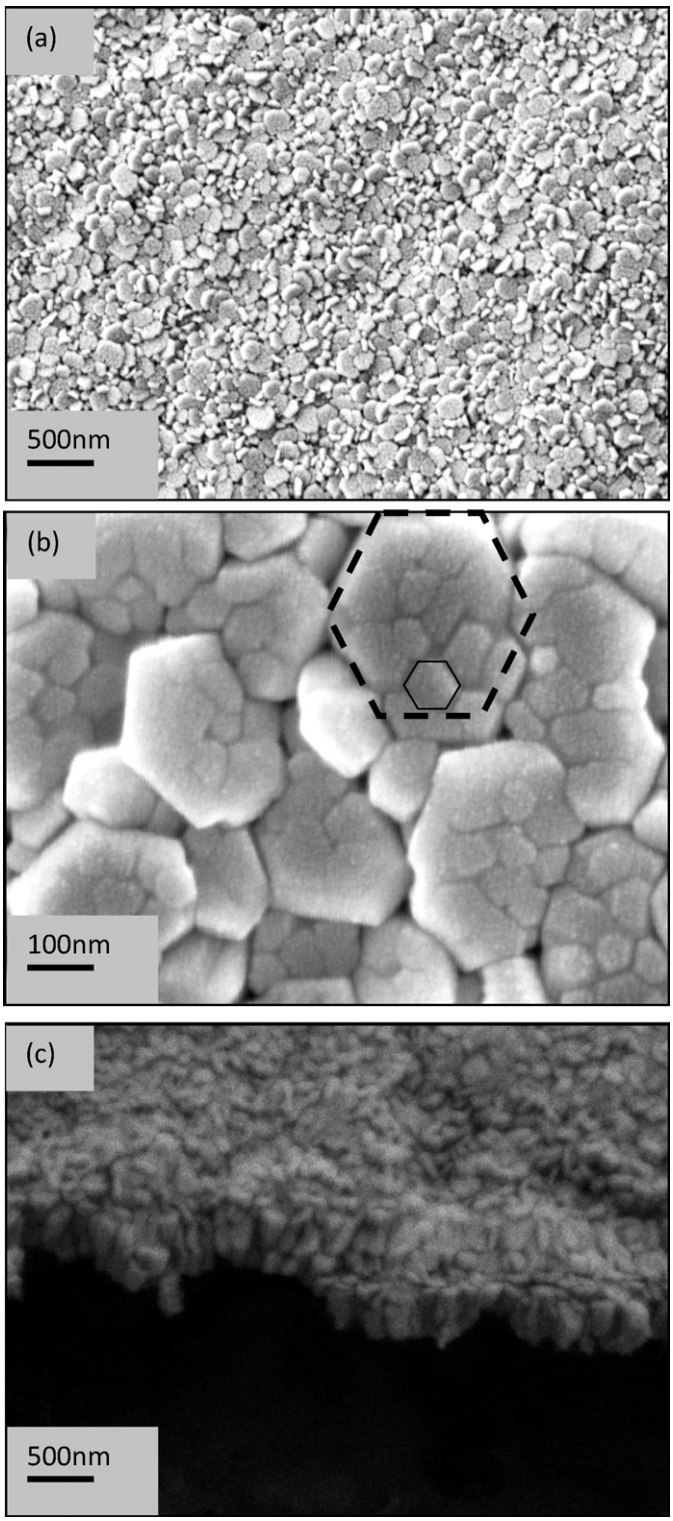

Fig. 1. Morphologies of Zn film deposited on PTFE sheet: (a) surface morphology at low magnification, (b) surface morphology at high magnification and (c) cross sectional view.

fast growing oxide at the side walls provides excellent nucleation sites for the ZnO formed from the vapour. As this process continues, randomly orientated whiskers emerge at the grain boundaries, forming the structure shown in Fig. 2(d).

Oxidised Zn films on PTFE in air and oxygen environment were subjected to X-ray diffraction analysis. As shown in Fig. 3, both samples exhibited 2θ peaks at 31.70°, 34.50° and 36.00°,

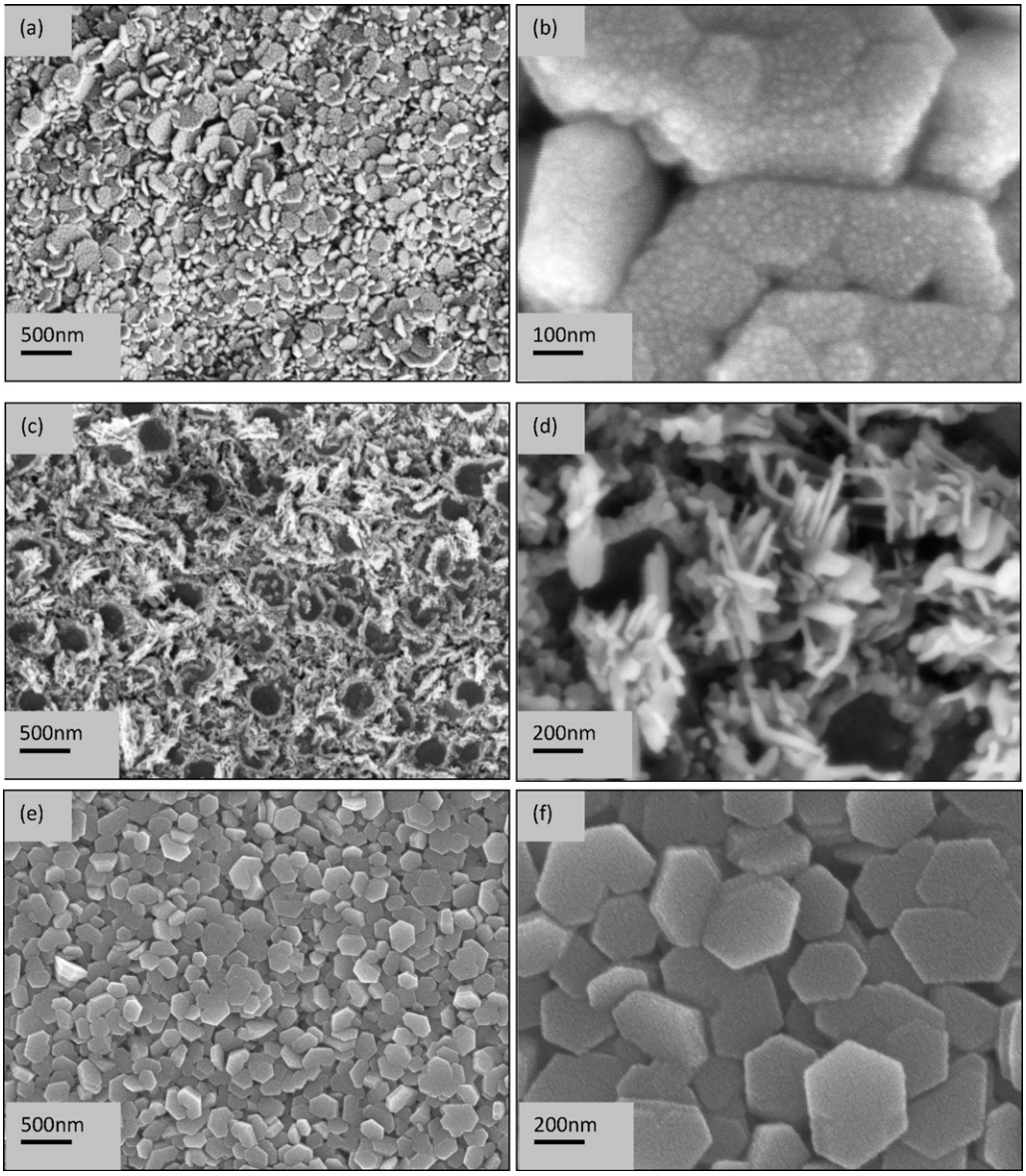

Fig. 2. Surface morphologies of oxidised Zn film on PTFE sheet: (a) low magnification (oxidation at 400 °C in air for 1 h), (b) high magnification (oxidation at 400 °C in air for 1 h), (c) low magnification (oxidation at 400 °C in oxygen for 1 h), (d) high magnification (oxidation at 400 °C in oxygen for 1 h), (e) low magnification (oxidation at 300 °C in air for 1 h) and (f) high magnification (oxidation at 300 °C in air for 1 h).

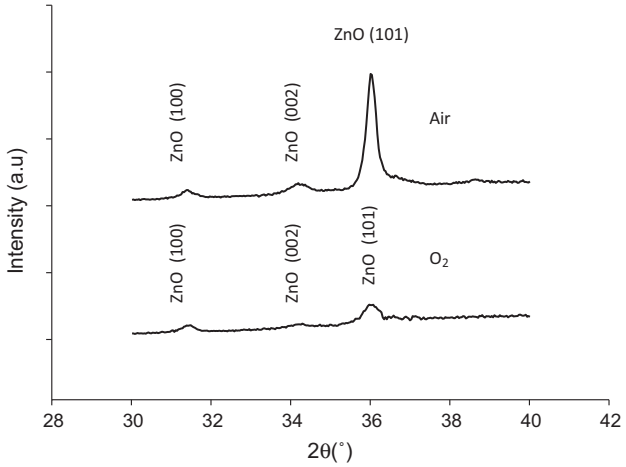

Fig. 3. XRD patterns of oxidised Zn layer on PTFE at 400 °C in air and oxygen for 1 h.

which correspond to (1 0 0), (0 0 2) and (1 0 1) ZnO, respectively (ICDD = 00-036-1451). The (0 0 2) peak of Zn was overlapping with the (1 0 1) ZnO peak for the oxidation in air. The sharp peak could be caused by both ZnO (1 0 1) and the (0 0 2) Zn from the underlying thermal evaporated Zn layer. The intensity of the Zn layer oxidised in O_2 was lower than oxidised in air because the underlying Zn layer was completely oxidised in excess oxygen condition. Therefore, the intensity of (0 0 2) Zn peak was eliminated and only ZnO (1 0 1) peak was detected. Note that the (1 0 1) ZnO peak overlaps the (0 0 0 1) Zn peak. Both of the films oxidised in air and oxygen consisted of wurtzite ZnO. Because the surface oxide formed at 400 °C was not very smooth and consisted of whisker grains, the oxidation temperature was reduced to 300 °C, and all oxidation was performed in air. The surface is thought to be adequate for use as the seed layer for the subsequent hydrothermal reaction of Zn ions. Typical morphologies of the surface oxide formed at 300 °C for 10 min are shown in Fig. 2(e) and (f) with low and high magnification images, respectively.

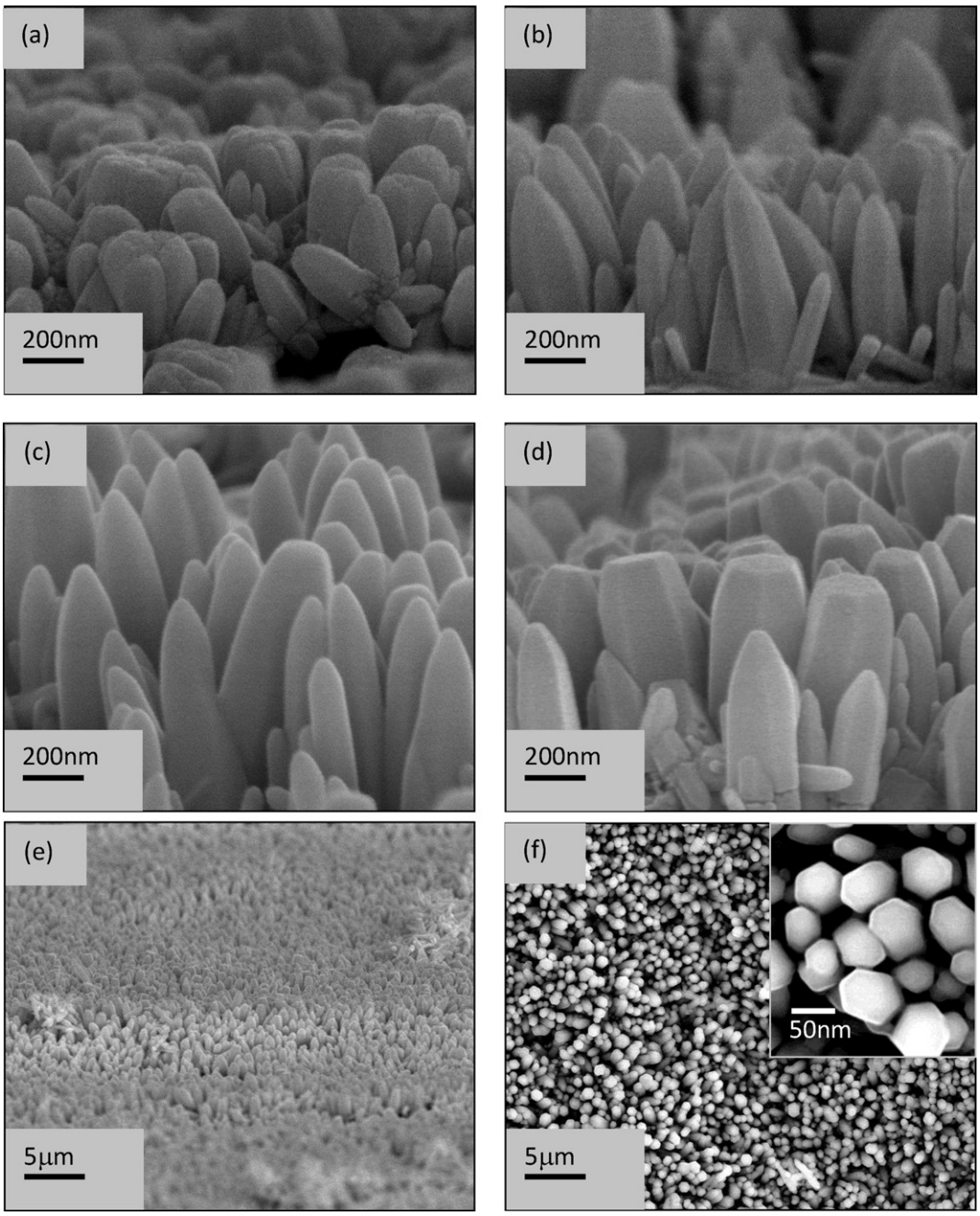

Fig. 4. Cross sectional morphologies of ZnO nanorods after hydrothermal reaction in reactive bath containing 0.1 M $Zn(NO_3)_2$ and 0.1 HMT (ratio of 1:1) at 80 °C for (a) 4 h, (b) 8 h, (c) 12 h and (d) 24 h; (e) low magnification of cross section of ZnO nanorods produced at 24 h; and (f) low and high (inset) magnifications surface morphology of ZnO nanorods produced by 24 h hydrothermal reaction.

3.2. ZnO nanorod array formation

Fig. 4(a)–(d) are the cross sectional images of the seeded PTFE sheet after hydrothermal reaction in the reactive solution consisting of HMT and Zn-ions (1:1 ratio) for 4, 8, 12 and 24 h, respectively. When compared to the morphology of the seed layer (Fig. 2(e) and (f)), it is obvious that the surface oxide changed to a rod-like structure after 4 h of hydrothermal reaction as shown in Fig. 4(a). The rods are around 100 nm long with a base diameter ranging from 30 nm to 100 nm. After 8 h of hydrothermal reaction in the reactive solution, the length of the rods was ~300 nm. The base diameter of the rods varied with the smallest rods having diameters of less than 30 nm and the largest ones having diameters of ~100 nm, as shown in Fig. 4(b). Most of the rods had sharp tips resembling needles. As the hydrothermal reaction time was increased to 12 h (Fig. 4(c)), more tapered rods formed, and the needle-like structure diminished. The base diameter of the rods became more uniform, averaging ~100 nm. The tip diameter was ~50 nm. The length of the rods was ~300 nm. After 24 h of hydrothermal reaction, hexagonal flat-top nanorods with well-defined angular walls were observed, as shown in the low magnification image of the sample in Fig. 4(e). The sample produced after 24 h of hydrothermal reaction became more uniform in terms of the distribution of the dimensions of the rods, which can be seen in the low magnification cross section morphology shown in Fig. 4(d). The base diameter was ~100 nm, and the tips of the rods were around 50 nm, as shown in the surface morphology in the inset of Fig. 4(f).

In a hydrothermal process, the vapour–liquid–solid (VLS) growth mechanism, which is often used to explain the formation of ZnO nanorods or nanowires in physical deposition processes, is not applicable [11]. Instead, the growth of the rods is thought to occur by a solid–liquid–solid (SLS) mechanism [11–14]. In the SLS mechanism, HMT plays an important role. Due to the nature of HMT, oriented growth of ZnO could occur. HMT hinders the growth of the six prismatic planes of the ZnO crystal and promotes the growth in the *c*-axis, and hence the rod-like structure is formed. Two important factors must be considered in the hydrothermal reaction of ZnO nanorods array formation: (a) adequate temperature for the decomposition of HMT and (b) the formation of ZnO nanocrystals at the early stage of the process.

The former factor is required because hydroxyl ions from thermally decomposed HMT (via reactions (1) and (2)) are required for ZnO formation [13]. Thermally decomposed HMT releases OH^- slowly in the bath until the solution reaches a supersaturation where Zn ions start to react with the OH^- to form $Zn(OH)_2$ as shown in reaction (3). $Zn(OH)_2$ decomposes to form ZnO. A temperature of 80 °C is thought to be an adequate temperature for HMT to decompose in the autoclave, while the starting pH of the solution was kept constant ~7 to avoid massive dissolution of the nanorods when higher pH is used [11–14]. However, too low of a pH would not allow reaction (2) to occur. The pH will however eventually increase as a function of hydrothermal reaction time.

$$C_6H_{12}N_4 + 6H_2O \leftrightarrow 6HCHO + 4NH_3 \quad (1)$$

$$NH_3 + H_2O \leftrightarrow NH_4^+ + OH^- \quad (2)$$

$$2OH^- + Zn^{2+} \leftrightarrow Zn(OH)_2 \quad (3)$$

$$Zn(OH)_2 \leftrightarrow ZnO + H_2O \quad (4)$$

Concerning the latter factor (which is the formation of ZnO nanocrystals), it is expected that the seed layer formed by the oxidation of the Zn film on PTFE sheets provides heterogeneous nucleation sites for ZnO formation. Seed layers proved to be crucial for the hydrothermal growth of the ZnO nanorods [11,15,16]. The seed layer facilitates the formation of ZnO nanocrystals at the early stage of growth. The nanocrystals prefer a perfect hexagonal structure. Assuming that all of the nanocrystals have this hexagonal structure, HMT as a non-ionic ligand chelates on the non-polar surface of ZnO nanocrystals on the six prismatic side planes of the wurtzite crystal and induces *c*-axis growth [11,17]. Radial enlargements of the rods are inhibited by the use of HMT as the chelating agent. As a polar crystal, each Zn atom is tetrahedrally coordinated to four O atoms and vice versa. Zn^{2+} and O^{2-} ion layers are arranged alternately along the *c*-axis or the [0 0 0 1] direction, which induces an accumulation of charges on the surface of the oxide either positively or negatively charged depending on the terminating atoms. The subsequent growth occurs only by the accumulation of $Zn(OH)_2$ or $Zn(OH)_2(NH_3)_4$ on the existing initial grains. Growth in the *a*–*b* planes is much reduced because the chelating of HMT of these sides retards the adsorption of Zn ions for further reactions to occur in these regions. Such a phenomenon only allows growth on the surface of the crystal along the [0 0 0 1] direction. XRD patterns for samples prepared for 4, 8, 12 and 24 h are shown in Fig. 5(a)–(d), respectively. As expected, for all samples, the diffraction patterns have a strong relative (0 0 0 1) intensity. The intensity of the (0 0 0 1) phase increased with increasing hydrothermal reaction time through 4, 8, 12 to 24 h. For ZnO produced for 24 h of hydrothermal reaction, as seen in Fig. 2(f), perfect hexagonal wurtzite rods can be seen, which clearly correspond to the (0 0 0 1) grains growth.

To demonstrate that the rods formed were indeed (0 0 0 1) ZnO crystals, HR-TEM images were obtained for the samples prepared for 12 h. An HR-TEM image of an individual rod is shown in Fig. 6(a).

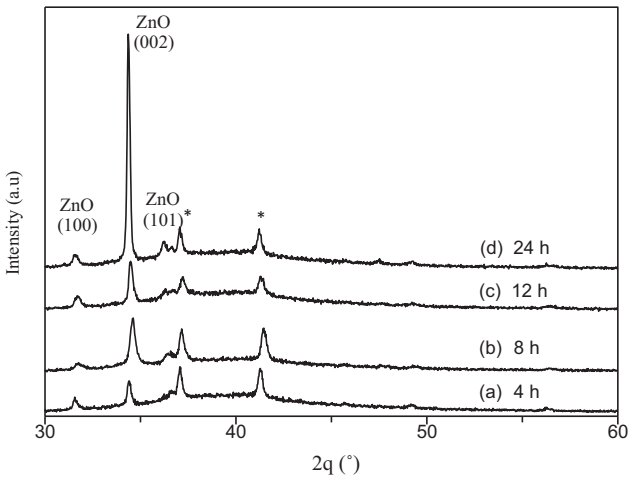

Fig. 5. X-ray diffraction patterns of ZnO nanorods formed in hydrothermal reactive bath containing 0.1 M $Zn(NO_3)_2$ and 0.1 M HMT at 80 °C for (a) 4 h, (b) 8 h, (c) 12 h, and (d) 24 h (* denotes peak from Zn).

In agreement with the SEM images, the nanorod has a smooth surface with a tip diameter of 50 nm and a base diameter of 100 nm. The needle-like morphology indicates the fast growth at the centre of the rods as opposed to the sides, confirming the chelating behaviour of the HMT. Fig. 6(b) is an HR-TEM image to show the general distribution of the nanorods, and in Fig. 6(c), a high magnification HR-TEM image is shown. The clear lattice fringes of 0.52 nm confirmed that the ZnO nanorods are single crystals with a ZnO wurtzite structure and an interplanar spacing of (0 0 0 1). In addition, the SAED pattern inset in the figure confirms the crystallinity of the rod. The HR-TEM image also shows that the ZnO nanorod is structurally uniform with no defects such as dislocations and stacking faults. These HR-TEM results are consistent with the XRD results that confirm that the ZnO grew predominantly at the (0 0 0 1) plane. The results are in agreement with Sugunan et al. [17].

Fig. 7 shows the Raman spectra for the sample prepared at 12 h. Single-crystalline ZnO has eight sets of optical phonon modes at the point of the Brillouin zone. Group theory predicts the existence of the following optic modes:

$$\Gamma_t = A_1 + 2B_1 + E_1 + 2E_2.$$

Both A_1 and E_1 modes are polar and can be divided into transverse (TO) and longitudinal optical (LO) phonons. Non-polar phonon modes with a symmetry of E_2 have two frequencies, E_2 (H), which is associated with oxygen atoms, and E_2 (L), which is associated with the Zn sublattice accordingly. Among all the optical modes, only the A_1, E_1 and E_2 modes are Raman active for ZnO single crystal material [18–20].

Three sharp peaks were detected at 331, 384, and 438 cm^{-1}. The peak at 438 cm^{-1} belongs to the high-E_2 mode of non-polar optical phonons, which corresponds to the characteristic band of the hexagonal wurtzite phase and further indicates nanorods with good crystal quality [18]. The peaks at 331 cm^{-1} and 384 cm^{-1} can be assigned to the $3E_{2H}$–E_{2L} and A_1 (TO) modes of ZnO, respectively [21]. In addition, the peaks at 384 cm^{-1} and 538 cm^{-1} correspond to A_1 (TO) and A_1(LO), respectively, and were similar to the results reported by other researchers [20]. The Raman peaks at 290 cm^{-1} and 730 cm^{-1} are attributed to the PTFE substrates and correspond to the symmetric stretching vibration of C–C and the torsion vibration of CF_2 [21]. Because the oxide is at the nanoscale, the vacancies were expected, especially around the boundaries of the oxide.

Fig. 8 is the photoluminescence plots of the nanorods formed at 4, 8, 12 and 24 h. For all samples, a strong UV emission peak can be seen at 380 nm. The UV emission peak can be attributed

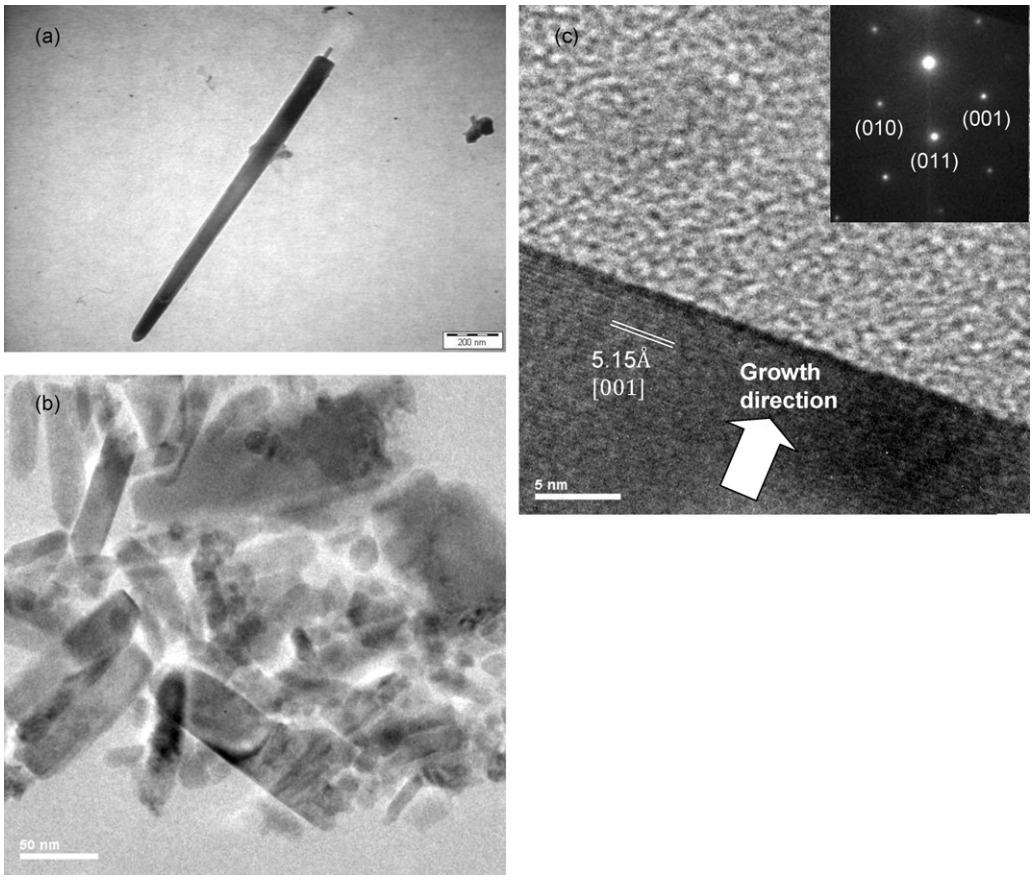

Fig. 6. Transmission electron micrographs for ZnO nanorods formed using hydrothermal reaction in 0.1 M $Zn(NO_3)_2$ and 0.1 HMT (ratio of 1:1) at 12 h. Images show (a) a single nanorod, (b) HR-TEM image of the nanorods and (c) high magnification image with an inset of selected area electron diffraction (SAED) pattern.

to the recombination of free excitons via band to band recombination [18,22], which also indicates good crystallinity of the ZnO nanorods obtained in agreement with the HR-TEM results. However, a peak associated with green emission was also observed at around 560 nm all the samples. This emission is attributed to the existence of oxygen vacancies referred to as deep-level or trap-state emission, and it could also be attributed to the excess of Zn ions in the rods. The optical band gap measured from these plots was at 3.2 eV on average.

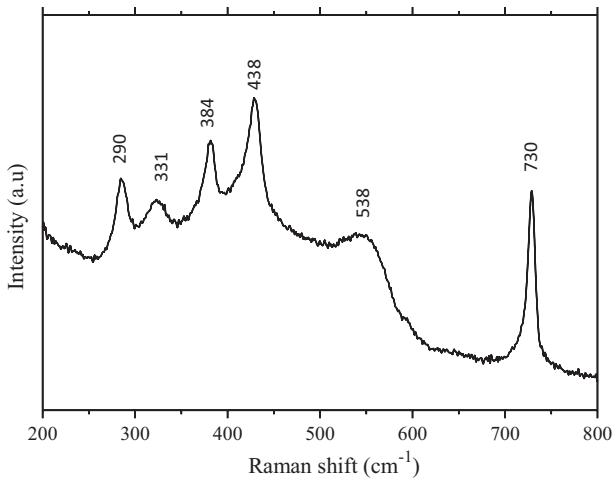

Fig. 7. Raman spectrum for hydrothermally grown ZnO nanorods on seeded PTFE at 80 °C for 12 h using molar ratio 1:1.

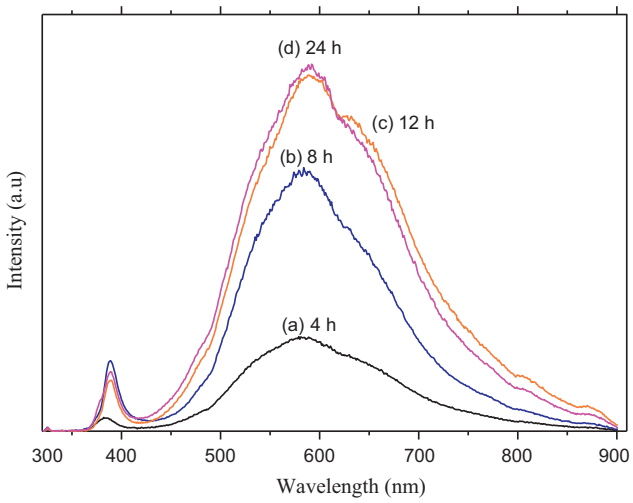

Fig. 8. Photoluminescence of ZnO nanorods formed in hydrothermal reactive bath for (a) 4 h, (b) 8 h, (c) 12 h and (d) 24 h.

4. Conclusion

Well aligned ZnO nanorod arrays were successfully formed on seeded PTFE sheets using the low-temperature hydrothermal method. XRD, HR-TEM and SAED analyses showed that the ZnO nanorods formed had the single-crystal wurtzite structure with a preferential growth plane of (0 0 0 1). PL measurement results showed two major peaks emission in the UV region and green region. The success in the formation of ZnO nanorod array on PTFE

was due to the use of HMT in the reactive solution, which was able to chelate the growing crystals at the *a*–*b* plane and promote growth at the polar surface along the *z*-direction. The growth promoted the growth of (0 0 0 1) ZnO. As the hydrothermal reaction time was increased from 4 h to 24 h, the nanorod arrays became much more uniform.

Acknowledgements

This work is supported by Fundamental Research Grant Scheme Fund (No. 6071164), Ministry of Higher Education, Malaysia, Universiti Sains Malaysia (USM) fellowship; USM-RU-PGRS (8031019), Research University grant (811069). The author (W.K. Tan) is now with the JENESYS programme at Toyohashi University of Technology, Japan under the supervision of Prof. Atsunori Matsuda. HR-TEM was conducted by Dr. Mat Hussain Salleh at Advanced Materials Research Centre, SIRIM Bhd. Malaysia.

References

[1] C.C. Myeon, K. Youngkhoo, H. Chang-Sik, Prog. Polym. Sci. 33 (2008) 581–630.
[2] S.-S. Kwon, W.-K. Hong, G. Jo, J. Maeng, T.-W. Kim, S. Song, T. Lee, Adv. Mater. 20 (2008) 4557–4562.
[3] U. Ozgur, Ya.I. Alivov, A. Teke, M.A. Reshchikov, S. Dogan, V. Avrutin, S.-J. Cho, H. Morkoc, J. Appl. Phys. 98 (2005) 1–103.
[4] S. Logothetidis, Mater. Sci. Eng. B 152 (2008) 96–104.
[5] Y. Liu, C. Pan, Y. Dai, W. Chen, Mater. Lett. 62 (2008) 2783–2786.
[6] Y.Y. Liu, Y. Yuan, X. Gao, S. Yan, X. Cao, X. Wei, Mater. Lett. 61 (2007) 4463–4465.
[7] C.-Y. Wong, L.-M. Lai, S.-L. Leung, V.A.L. Roy, Mater. Sci. Eng. B 164 (2009) 80–84.
[8] S.-H. Yi, S.-K.C. Choi, J.-M. Jang, J.-A. Kim, W.-G Jung, J. Colloid Interface Sci. 313 (2007) 705–710.
[9] F. Li, Z. Li, F. Jin, Physica B 403 (2008) 664–669.
[10] C.F. Guo, Y. Wang, P. Jiang, S. Cao, J. Miao, Z. Zhang, Q. Liu, Nanotechnology 19 (2008) 445710.
[11] Z. Lockman, P.F. Yeo, W.K. Tan, K. Ibrahim, K. Abdul Razak, J. Alloy Compd. 493 (2010) 699–706.
[12] L.Z. Pei, H.S. Zhao, W. Tan, H.Y. Yu, Y.W. Chen, C.G. Fan, Q.-F. Zhang, Physica E 42 (2010) 1333–1337.
[13] M.N.R. Ashfold, R.P. Doherty, N.G. Ndifor-Angwafor, D.J. Riley, Y. Sun, Thin Solid Films 515 (2007) 8679–8683.
[14] S. Baruah, J. Dutta, J. Cryst. Growth 311 (2009) 2549–2554.
[15] S. Baruah, J. Dutta, J. Sol-Gel Sci. Technol. 50 (2009) 456–464.
[16] S.-F. Wang, T.-Y. Tseng, Y.-R. Wang, C.-Y. Wang, H.-C. Lu, Ceram. Int. 35 (2009) 1255–1260.
[17] A. Sugunan, H.C. Warad, M. Boman, J. Dutta, J. Sol-Gel Sci. Technol. 39 (2006) 49–56.
[18] R. Zhang, P.-G. Yin, N. Wang, L. Guo, Sol. State Sci. 11 (2009) 865–869.
[19] Y. Wang, X. Li, G. Lu, X. Quan, G. Chen, J. Phys. Chem. C 112 (2008) 7332–7336.
[20] S.P. Firsov, G.R. Zhbankov, M. Bakhramov, A. Abdukadyrov, A. Gafurov, J. Appl. Spectrosc. 59 (1993) 3–4.
[21] W.I. Park, Y.H. Jun, S.W. Jung, G.-C. Yi, Appl. Phys. Lett. 82 (2003) 964–971.
[22] J.P. Kar, M.H. Ham, S.W. Lee, J.M. Myoung, Appl. Surf. Sci. 255 (2009) 4087–4092.